Available online at www.sciencedirect.com
SCIENCE DIRECT®
Nuclear Instruments and Methods in Physics Research A 553 (2005) 18–24
NUCLEAR INSTRUMENTS & METHODS IN PHYSICS RESEARCH Section A
www.elsevier.com/locate/nima

Novel Cherenkov photon detectors

Fabio Sauli*

CERN, Geneva, Switzerland

Available online 22 August 2005

Abstract

Gaseous detectors using multiple gas electron multiplier (GEM) electrodes permit to attain large amplification factors with a strong suppression of photon and ion-mediated feedback. With the first GEM in a cascade coated with a photosensitive layer, they provide efficient and fast single photon detection, with excellent position resolution. General performances of CsI-coated multi-GEM detectors are described, as well as a promising method of signal readout, the so-called hexaboard, a matrix of interconnected pads that permits to achieve ambiguity-free reconstruction of multi-photon events, a major requirement for RICH applications.
© 2005 Elsevier B.V. All rights reserved.

PACS: 29.40.ka

Keywords: Cherenkov photon detectors; RICH; Gas electron multiplier (GEM)

1. Introduction

The gas electron multiplier (GEM) is a thin, metal-clad polymer foil, chemically etched with a high density of narrow holes, typically 50–100 mm^{-2} (Fig. 1) [1]. On application of a voltage between the conducting sides, each hole acts as an independent proportional counter: electrons released in the gas volume drift into the channels, multiply in avalanche and transfer into the following region. Several foils can be cascaded (Fig. 2); the avalanche confinement in the holes results in efficient ion- and photon-mediated feedback suppression, and permits to attain very large gains [2].

The multiplying electrodes are electrically separated from the charge-collecting anode plane: this protects the readout electronics from accidental discharges and permits a wide freedom in the design of the readout pattern, pads or strips of arbitrary shapes.

GEM-based detectors operate efficiently at very high particle fluxes, up to 1 MHz mm^{-2}, are robust and immune from radiation-induced aging deterioration up to very high integral fluxes [3].

*Corresponding author at: Gas Detector Development, EP Division, CERN, 1211 Geneva 23, Switzerland. Tel.: +41 22 7673670; fax: +41 22 7677100.
E-mail address: fabio.sauli@cern.ch.

0168-9002/$ - see front matter © 2005 Elsevier B.V. All rights reserved.
doi:10.1016/j.nima.2005.08.024

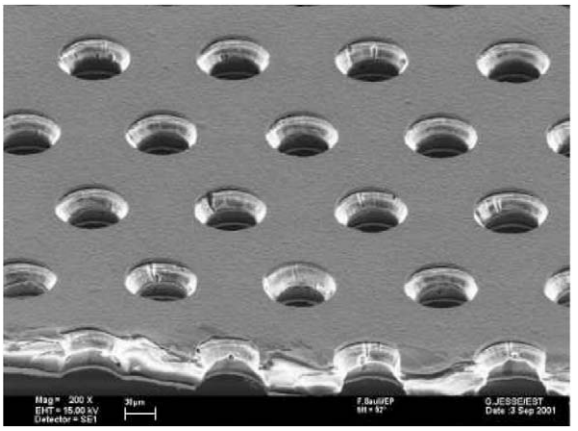

Fig. 1. Electron microscope view of a GEM. Hole diameter and pitch are 70 and 140 μm.

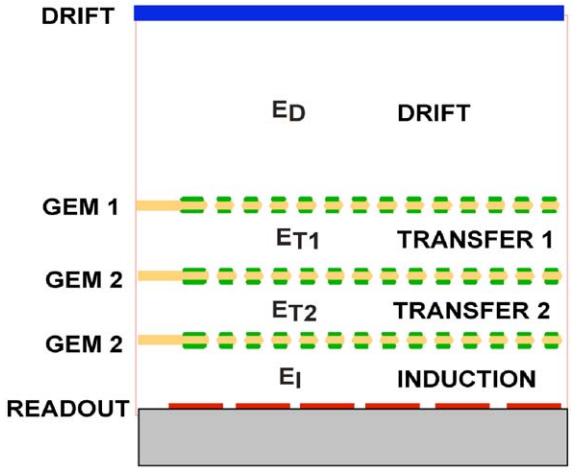

Fig. 2. Schematics of a triple-GEM detector.

Offering position accuracies of 50 μm and multi-particle resolutions of around 1 mm, they are already in use in several particle physics experiments or under development for other applications. Fig. 3 shows one of the triple-GEM detectors built for the COMPASS experiment at CERN; 20 chambers, with an active area of $\sim$1000 cm^2 each and two-dimensional projective readout, are successfully operated in the experiment [4]. Fig. 4 is a close view of a prototype for the TOTEM forward tracker for CMS, of similar conception but with a shape tailored to detect particles very close to the primary beam [5]. A system of 40 semi-circular detectors providing both accurate radial coordinates of tracks and a fast geometrical trigger at the high rate and event multiplicity of the experiment is in construction.

For a review of applications of GEM-based devices in various fields see for example Ref. [6].

2. Detection of photons

GEM detectors can be made sensitive to photons using an internal photosensitive layer,

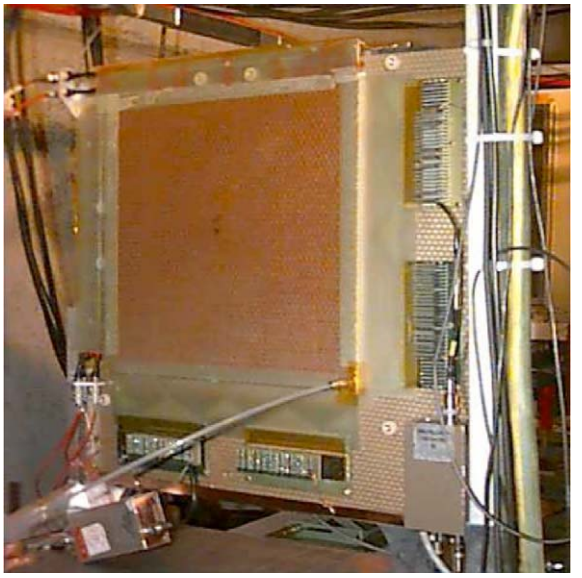

Fig. 3. Triple-GEM detector for COMPASS; the active area has about 1000 cm^2.

Fig. 4. Prototype of a GEM detector for TOTEM.

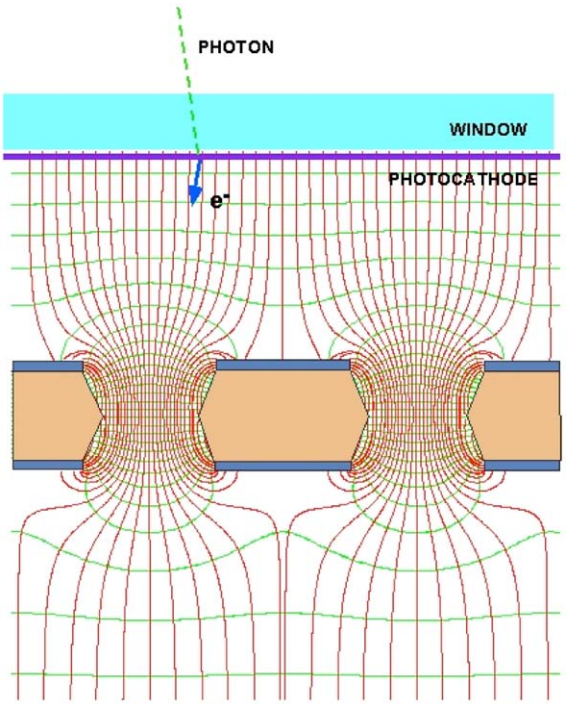

Fig. 5. Schematics of a GEM detector with transmission photocathode.

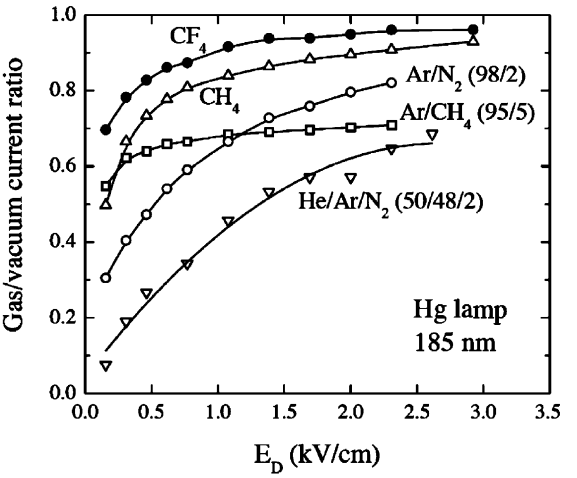

Fig. 6. Photoelectron collection efficiency, relative to vacuum, for a CsI photocathode.

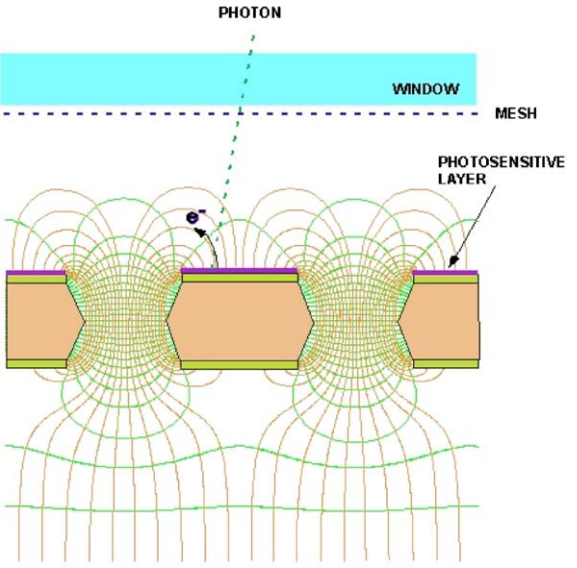

Fig. 7. GEM detector with absorption photocathode.

deposited on the inner side of the window (Fig. 5). Ejected photoelectrons are drifted into the first GEM, amplified in a cascade of multipliers and detected on a patterned charge-collecting electrode. Most recent work has been done using thin CsI photocathode layers, sensitive in the ultraviolet wavelengths below 210 nm. Due to a process of backscattering by the gas molecules, the effective detection efficiency, compared to vacuum, depends on gas filling and electric field strength at the surface of the cathode.

Fig. 6 shows the anodic current, measured on a triple-GEM detector with a transmission CsI photocathode, normalized to vacuum and for constant illumination [7]; methane and carbon tetra-fluoride are a convenient choice for obtaining good efficiency at moderate voltages.

An attractive option is to deposit a reflective photocathode on the upper GEM electrode, facing the window (Fig. 7) [8,9]. The high surface field on the area surrounding the holes permits to efficiently extract photoelectrons, and to inject them into the cascade of multipliers. A reverse field applied to the drift region eliminates the contribution of ionization by charged particles in the gap, an essential advantage in RICH counters. With this geometry, photon feedback from the ava-

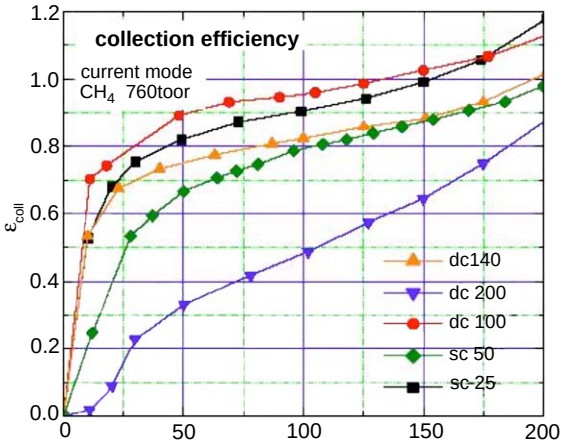

Fig. 8. Photoelectron collection efficiency, relative to vacuum, for several GEM geometries.

lanches is absent altogether; as most of the charge is produced in the last stage, ion feedback is also strongly reduced. Systematic studies on the effect of GEM geometry and operating voltage on the photoelectron extraction probability are described in Ref. [10]; as shown in Fig. 8, from the quoted work, the best results are obtained with narrow holes at small pitch.

Promising developments are also on the way to manufacture sealed multi-GEM devices, thus permitting the use of alkali photocathodes sensitive in the visible region [10]. As ion bombardment can easily damage the sensitive photocathodes, detailed studies on various ways to reduce the fraction of ions reaching back have been performed, by optimized design and choice of fields. Introduction of a gating electrode, pulsed in synchronism with the transit of the positive ions produced in the avalanche, eliminates the feedback problems [11]; the method is however rate-limited and cumbersome to use. Alternate detector geometries such as the Micro-hole and Strip allow to substantially reduce the fraction of ions reaching the photocathode [12].

3. Photon localization accuracy

The single photon localization properties of a medium-size triple-GEM detector with reflective photocathode have been investigated with a small multi-GEM detector, having an active area of $10 \times 10\,\mathrm{cm}^2$ and projective one-dimensional strip readout on the anode [13]. The first GEM electrode, facing the window, was coated with a thin layer of CsI[1]. Transfer and induction gaps in the detector were 2 mm thick, with a 3-mm-thick drift region; a 5-cm-diameter UV-grade quartz widow permitted exposing the central part of the detector to UV photons, through the upper drift electrode made with a thin mesh. Although we could not verify directly the quantum efficiency, there is at CERN a considerable experience in producing large area photocathodes, for example for the COMPASS RICH [14].

After completion, the detector is mounted on an optical bench supporting the photon source and the collimators; a micrometer permits to accurately displace the chamber in front of a collimated photon beam for position and linearity measurements. As source, we have used discharges in a glass vessel containing low-pressure hydrogen; energy and frequency of the discharges are controlled by external circuitry. A capacitive pickup on the lamp provides the discharge time, used for measurements in coincidence; a collimator and a set of filters controlled size and intensity of the beam. Charge signals were recorded on eight adjacent readout strips, at 200 μm pitch, using low-noise amplifiers followed by gated charge ADCs.

As filling-gas we have used pure methane transparent to photons between the CsI quantum efficiency threshold (~6.2 eV) and the window cut-off (~7.5 eV). Powered with a standard resistive divider, the detector was operated with equal potentials (515 V) across the three GEMs, and equal fields (~4.6 kV/cm) in the transfer and induction gaps; the drift potential was equal or slightly lower than the one applied to the photocathode.

Fig. 9 shows pulse height spectra obtained, reducing progressively the UV source intensity, recorded at constant detector gain and equal number of coincidence signals from the lamp. The spectra have an exponentially decreasing shape; single photon counting is demonstrated by

[1]By the CERN Thin Film section (A. Braem).

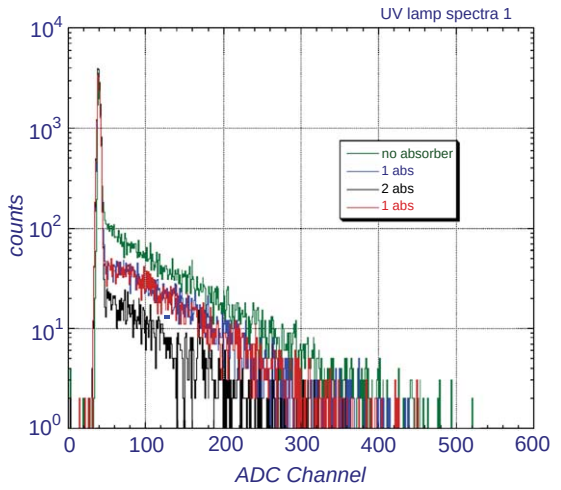

Fig. 9. Single photoelectron pulse height spectra.

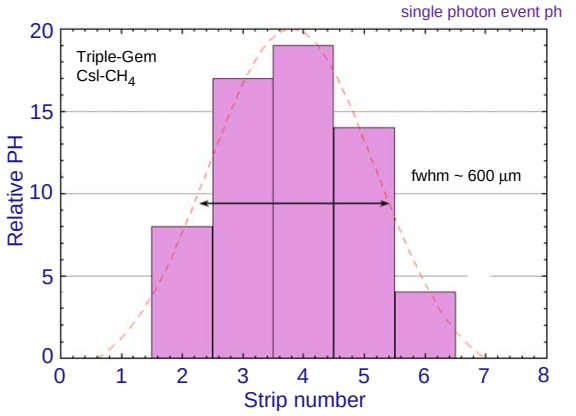

Fig. 10. Induced charge profile for a single electron avalanche. Strip pitch 200 μm.

the reduction in integral count with an identical shape.

Fig. 10 gives an example of recorded distribution of charge for a single electron avalanche; it has a FWHM of 600 μm. Because of the limited region equipped with electronics (eight strips, or 1.6 mm) we could not directly study the two-photon resolution, but the width of the distribution should allow to disentangle two hits about 1 mm apart, an essential feature in view of RICH applications.

The distribution of centre of gravity of the detected charge in each event, recorded for two positions 200 μm apart, has an FWHM of 160 μm (Fig. 11); subtracting the estimated source width (100 μm) we can infer a single photon localization accuracy around 125 μm FWHM (~ 55 μm rms). Displacing with a micrometer the detector in the direction perpendicular to the strips, we have recorded around 1000 events per position and computed the corresponding centre of gravity distributions. Fig. 12 shows the correlation between geometrical position and computed centre of gravity; within the range of the scan, about 0.5 mm, the correlation is linear within errors.

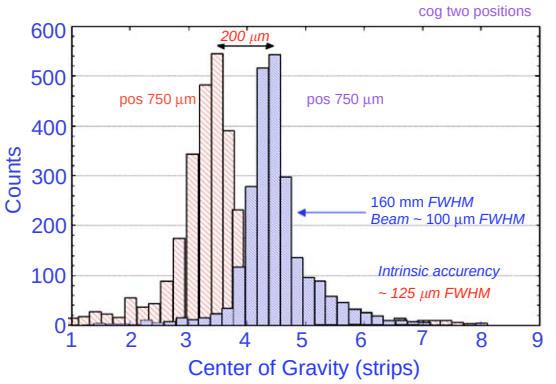

Fig. 11. Centre of gravity distribution for two collimated photon beams 200 μm apart.

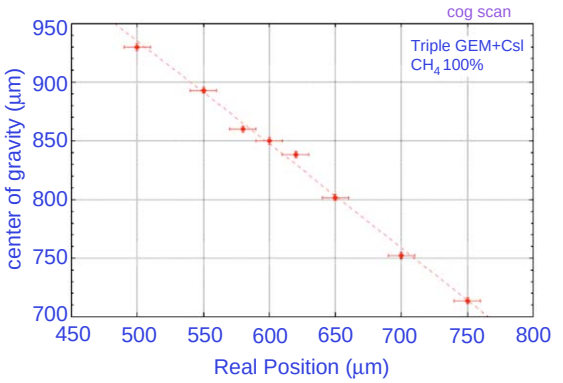

Fig. 12. Correlation between real and measured position for single photoelectrons.

4. Hexaboard readout

For the previous study we used a single set of parallel strips. Two-dimensional projective readout of coordinates can be obtained using perpendicular strips; for moderate multiplicities, the correlation between the charges recorded on the projections can be used to resolve ambiguities arising for multi-hit events [4]. A 2-D projective strip readout is, however, not suitable for the spatially close multi-photon events in RICH applications. The ultimate multi-hit resolution can be achieved using as pick-up electrode a matrix of pads, independently read out; this is however a very expensive proposition. An elegant alternative, with performances between projective strips and pixel readout, has been developed under the name "hexaboard"; it consists in a matrix of adjacent charge collecting hexagonal pads, interconnected in rows along three directions at 120° to each other [15]. For each event, three independent charge profiles are recorded, providing an ambiguity-free reconstruction up to large multiplicities; charge correlation adds to the resolution power.

To investigate its performance in the detection of photons, we have built a detector with a hexagonal-shaped hexaboard anode plane (Fig. 13) [16]. The device has 170 readout channels for each of the three projections, each channel providing the signal from a row of interconnected hexagonal pads at a pitch of 520 μm. A set of four framed GEM foils, with $10 \times 10\,\mathrm{cm}^2$ active area, were mounted over the padded anode on insulating pillars; the upper side of the first GEM, facing the UV-transparent quartz window, was coated with CsI as described. Only 48 strips (16 in each of the three projections) were equipped with a charge recording circuit, an integrated fast amplifier followed by the a highly integrated ADC system developed for the ALICE time projection chamber (ALTRO [17]). Typically, the charge is shared between two adjacent rows, therefore permitting charge interpolation in the calculation of the coordinates; the cluster width in all coordinates has ~250 μm rms.

Using a mask with several holes, we have studied the resolution properties of the detector for multi-photon events; Fig. 14 shows, as an example, signals recorded along the three projections for a double photon event. As in the detection of charged particles, we observe a strong correlation between charges recorded on the three projections, that can be used for reconstruction; Fig. 15 gives, as an example, the correlation between one pair; similar plots are obtained for the other pairs. Due to the wide spread in amplitude, charge correlation appears a very

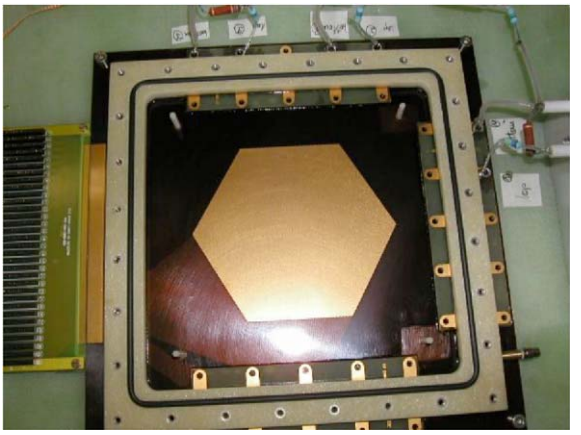

Fig. 13. GEM detector with hexaboard readout.

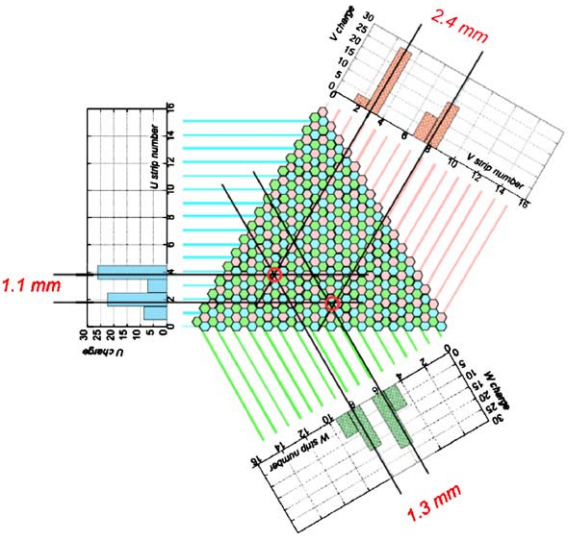

Fig. 14. Two-photon event recorded with the hexaboard GEM detector.

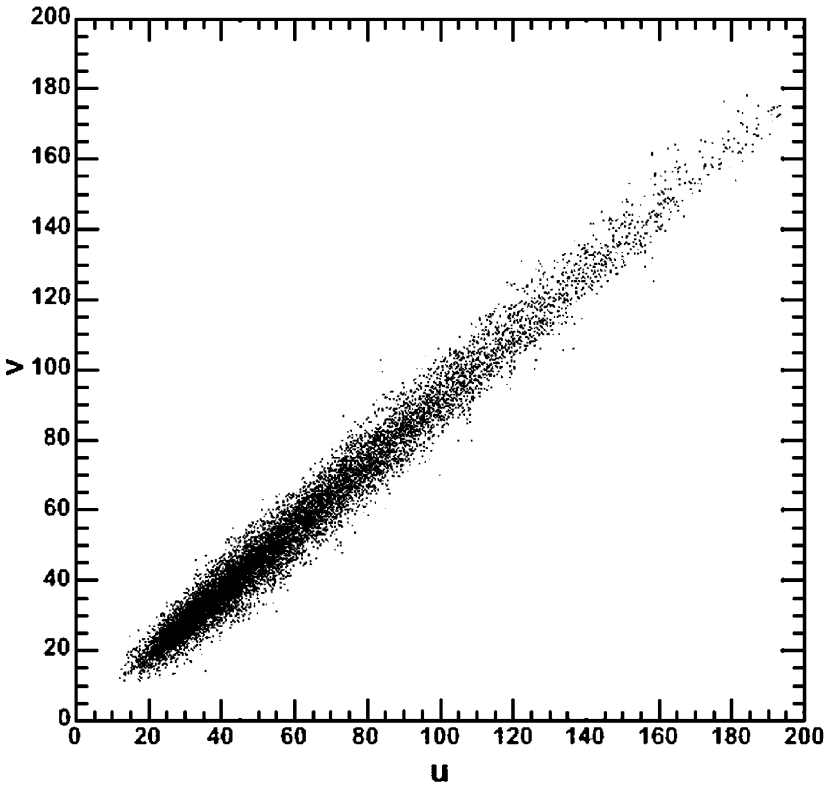

Fig. 15. Cluster charge correlation between two projections (arbitrary units). In the proof, there is enough space for the addition without an increase in page counts.

powerful tool for the resolution of ambiguities in high-multiplicity events.

With a few ns time resolution, 100 μm position accuracy, two-points resolution around 1 mm and ambiguity-free multi-photon reconstruction, the GEM detector with hexaboard readout is a promising tool for the realization of fast RICH detectors.

References

[1] F. Sauli, Nucl. Instr. and Meth. A 386 (1997) 531.
[2] S. Bachmann, et al., Nucl. Instr. and Meth. A 438 (1999) 376.
[3] C. Altunbas, et al., Nucl. Instr. and Meth. A 515 (2003) 249.
[4] B. Ketzer, et al., Nucl. Instr. and Meth. A 535 (2004) 314.
[5] M. Bozzo, et al., Proceedings of the IEEE Nuclear Science Symposium, 16–22 October 2004, Rome.
[6] F. Sauli, Nucl. Instr. and Meth. A 522 (2004) 93.
[7] A. Breskin, et al., Nucl. Instr. and Meth. A 483 (2002) 670.
[8] R. Bouclier, et al., IEEE Trans. Nucl. Sci. NS-44 (1997) 646.
[9] D. Mörmann, et al., Nucl. Instr. and Meth. A 478 (2002) 230.
[10] D. Mörmann, et al., Nucl. Instr. and Meth. A 530 (2004) 258.
[11] D. Mörmann, et al., Nucl. Instr. and Meth. A 516 (2004) 315.
[12] J.M. Maia, et al., Nucl. Instr. and Meth. A 523 (2004) 334.
[13] T. Meinschad, et al., Nucl. Instr. and Meth. A 535 (2004) 324.
[14] E. Albrecht, et al., Nucl. Instr. and Meth. A 502 (2003) 112.
[15] S. Bachmann, et al., Nucl. Instr. and Meth. A 478 (2002) 104.
[16] F. Sauli, et al., Proceedings of the IEEE Nuclear Science Symposium, 16–22 October 2004, Rome.
[17] B. Mota, et al., Nucl. Instr. and Meth. A 535 (2004) 500.